Hindawi
Geofluids
Volume 2022, Article ID 5697710, 12 pages
https://doi.org/10.1155/2022/5697710

Research Article

A New Bayesian Network Model for the Risk Assessment of Water Inrush in Karst Tunnels

Yingchao Wang ,[1,2] Yang Liu ,[1] Zhaoyang Li,[2] and Wen Jiang[2]

[1]*State Key Laboratory for Geomechanics and Deep Underground Engineering, China University of Mining & Technology, Xuzhou, Jiangsu 221116, China*
[2]*State Key Laboratory of Geomechanics and Geotechnical Engineering, Institute of Rock and Soil Mechanics, Chinese Academy of Sciences, Wuhan 430071, China*

Correspondence should be addressed to Yingchao Wang; wangyingchao@cumt.edu.cn and Yang Liu; tb19220012b4@cumt.edu.cn

Received 22 December 2021; Accepted 30 April 2022; Published 14 June 2022

Academic Editor: Tao Chen

Water inrush seriously restricts the safe construction of a karst tunnel. Once it occurs, it will cause serious consequences such as economic loss and casualties. Due to the complexity of an underground environment, it is difficult to calculate the probability of karst tunnel water inrush. Therefore, it is of great engineering significance to establish an effective risk assessment model. Based on the Bayesian theory, interpretation structure model, and generative adversarial network, a Bayesian network risk assessment model is established. The results show that firstly, twelve indexes selected can not only characterize the karst tunnel water inrush but also are easy to be counted, which effectively improves the accuracy of the Bayesian risk assessment model. Secondly, the Bayesian network risk assessment model overcomes the shortcomings of other risk assessment models that rely too much on geological data and improves the accuracy through massive data training. Thirdly, the corresponding noninrush samples are generated by the generative adversarial network and analytic hierarchy process, which effectively solve the problem of an unbalanced database. Finally, the Bayesian network risk assessment model is applied to the DK490+373 section of the Shangshan Tunnel. The assessment model is operable, effective, and practical, and it is also suitable for the situation of incomplete index statistics.

1. Introduction

In recent years, with the development of underground engineering, the scale and difficulty of tunnel construction in China have leapt to the number one in the world. China, with an expanse territory, complex topography, climatic condition, and abundant karst landform, complex environment leads to water inrush disasters that frequently occur during the construction of underground engineering. According to statistics, water inrush accounts for about 40% of all kinds of disasters and nearly 50% of tunnel water inrush disasters are directly or indirectly caused by the karst landform, which seriously affects the safety of underground engineering construction, causing massive casualties and economic losses. Water inrush also leads to collapse, surface subsidence, water resources depletion, and other secondary disasters. Figure 1 shows the situation of water inrush in the Yesangaun Tunnel. On the 5th of August, 2007, water inrush occurred during the excavation and the quantity reached $15.1 \times 10^4\ m^3/d$, resulting in 10 deaths and half a year's delay of construction [1]. Therefore, it is of great engineering significance to establish an effective risk assessment model for water inrush probability and disaster consequences.

A long time ago, many experts and scholars have realized the danger of water inrush and which is easy to occur during the excavation in a karst stratum. In 1970s, for the first time, the British scholar Wilson J.L. [2] summarized

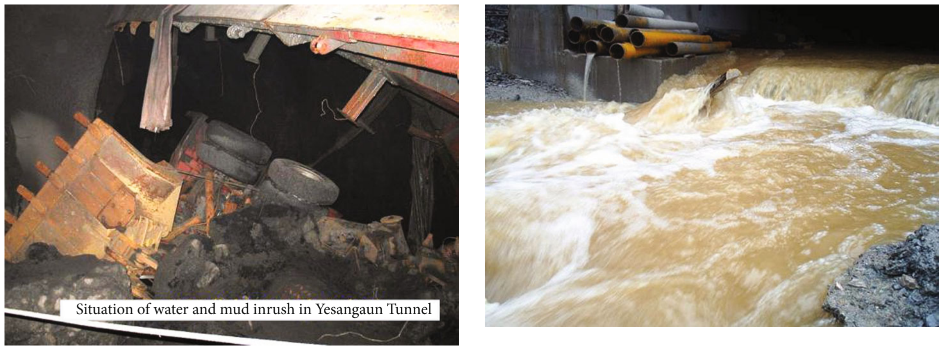

(a) (b)

Figure 1: Situation of water and mud inrush in the Yesangaun Tunnel [1].

the water inrush law of karst landform. Subsequently, in terms of theoretical research, scholars have carried out research on the disaster-causing mode and mechanism of water inrush in the karst tunnel through fluid mechanics, groundwater dynamics, rock mechanics, and fracture mechanics [3–6]. In addition, numerical simulation, experiment, and other methods are also introduced into the study about water inrush of the karst tunnel [7–13] carried out research on the occurrence mechanism, failure modes, and main influencing factors of water inrush in karst tunnels. Li et al. [14] divided the source of water inrush into three categories, cavity, fissure, and pipeline according to the type of karst structure, and pointed out that the development of disaster source was controlled by various factors such as geographic and geomorphic conditions and rock strata dip angle.

Based on the research about water inrush in a karst tunnel, the water inrush mechanism of the karst tunnel is complex and there are many influencing factors, which seriously affect the safety of underground engineering construction. Therefore, it is of great engineering significance to establish an effective risk assessment model for water inrush. The research about water inrush in the karst area lays a good foundation for the development of the water inrush risk assessment model of the karst tunnel. Based on the research about water inrush in a karst tunnel, the idea of risk assessment was firstly introduced into engineering in 1983 [15] and the first risk assessment model was established. Subsequently, three-dimensional reticulated exploration, GIS, case analysis, advanced geological prediction, Dempster-Shafer (D-S) evidence theory, microseismic monitoring technology, MFIM, TOPSIS, and other theories have been introduced into the risk assessment model [16–23].

In 1992, for the first time, Nilsen [24] implemented the risk assessment in the construction of a subsea tunnel and established the corresponding risk assessment model. Subsequently, Kampmann et al. [25] further extended the risk assessment method to the construction of subway engineering and formulated corresponding risk control measures. Weiss and Vig [26] extended the idea of risk assessment to the preliminary engineering design. Wang et al. [27, 28] introduced the efficiency coefficient method and analytical comparison method into the risk assessment model, which improved the calculation efficiency. Hou et al. [29] combined the AHP method and coefficient of variation method to the comprehensive weight and introduced the ideal point method.

At present, the risk assessment model has proved its effectiveness in underground engineering construction. However, most of the risk assessment models used for water inrush are based on detailed geological data and clear disaster causes. The complexity of the tunnel geological environment and the uncertainty of each index are ignored. Without detailed geological data as support, the accuracy of assessment model will be greatly reduced. And underground engineering itself has great fuzziness, and geological data collection is very difficult. Therefore, a new risk assessment model based on the Bayesian network theory is established, which effectively overcomes these problems. Bayes' theory has its origins in Bayes' 1763 work. The essence of Bayesian theory is to determine the mutual influence among various factors through data training and measured by probability, which can dynamically control the probability from the "macrolevel [30]". Therefore, the Bayesian theory is often used in engineering risk assessment models. Kool et al. [31] used the Bayesian theory to advance the procedure of hindcasting of levee failures and verified the dam failure near Breitenhagen in Germany. Zhao et al. [32] proposed a Bayesian method to effectively develop regional correlation models to estimate the runoff distance. This method systematically integrates the sparse data collected in a specific region and the prior knowledge embedded in the existing relevant models in other regions. The method is illustrated by examples and numerical examples. In order to better understand groundwater dynamics and improve the reliability of model prediction, Yin et al. proposed a Bayesian multimodel uncertainty quantification framework to explain the model parameter uncertainty in complex alluvial groundwater modeling. The method is applicable to the agricultural intensive Mississippi River alluvial aquifer (mraa) in Northeast Louisiana. Wu et al. proposed an integrated model based on dynamic hazard scenario identification (DHSI), Bayesian network (BN) modeling, and risk analysis for risk assessment of urban public utility tunnels. The worst-case scenario of urban utility tunnel accidents is identified by DHSI and modelled by BN. In 2014, for the first time, the Bayesian network was applied to the risk assessment model of tunnel construction. Hu [33] applied the Bayesian network to the stability assessment of the tunnel and proved the validity of his risk assessment model by monitoring displacement and stress.

Compared with other assessment models, the Bayesian risk assessment model established in this paper can accurately predict the water inrush of a karst tunnel through massive data training under the condition of incomplete geological data and unknown disaster cause. The selected evaluation indexes are more in line with the characteristics of the karst tunnel. In order to solve the problem that the Bayesian risk assessment model needs massive data training, for the first time, the idea of the generative adversarial network and the principle of the analytic hierarchy process are used to solve the problem of unbalanced database. The Bayesian network theory is of great theoretical significance to the risk assessment and disaster prevention of tunnel water inrush and to guide the safe and economic construction of a karst tunnel.

2. The Construction of the Bayesian Network Model

2.1. The Basic Principle of the Bayesian Network. Bayesian network is a probabilistic graph model that consists of nodes, directed arrows, and conditional probability table. Nodes represent random variables in the network, directional arrows represent the relationship between nodes, and conditional probability tables represent the degree of mutual influence between nodes. The Bayesian network has the following advantages: the statistical data are quantitatively evaluated, and the final results are determined according to the interval membership degree of each node. As the accumulation of statistical data, model evaluation can become more and more accurate without changing the original topology diagram. Be able to combine expert experience with training data.

The mathematical formula and the expression of conditional independence criterion of the Bayesian network are shown in formula (1) [34]:

$$P(M|N=a)=\frac{P(M)P(N=a|M)}{P(N=a)}. \tag{1}$$

In the formula, $P(M|N=a)$ is the posterior probability, which is the probability of M occurring when a new value of N is known as a; $P(M)$ is the prior probability, the probability of M before considering the new value of N, which is obtained by historical data; $P(N=a|M)$ is the likelihood of M, calculated from historical data; $P(N=a)$ is the probability that N is a.

2.2. Model Building Method. The widely used hybrid modeling method is adopted to build the model. The hybrid modeling method can integrate the influence relationship between the variables from experience into the data training without unnecessary causality, which can greatly improve the learning efficiency. The main steps of the hybrid modeling method are as follows. Firstly, representative evaluation factors of karst tunnel water inrush are selected and classified according to the risk classification. Secondly, the corresponding interpretation structure model is constructed and the evaluation index is processed hierarchically according to the influence relationship. Thirdly, according to the causality diagram method, the causal relationship of each node is modified.

Table 1: Risk classification of formation lithology.

Risk classification	$t=\sum A_iB_j$	Definition
I	>0.254	Strong karst stratum
II	0.104~0.254	Moderate karst stratum
III	0.042~0.104	Weak karst stratum
IV	<0.042	Nonsolute stratum

2.3. Selection of Evaluation Indexes. The influencing factors of water inrush in a karst tunnel can be summarized into geological factors, hydrological factors, and anthropogenic factors, through reviewing the relevant literature on the risk assessment of water inrush in a karst tunnel [5, 27, 28]. Six evaluation indexes are selected from geological factors, including topography and geomorphology, attitude of rocks, formation lithology, unfavorable geology, interlayer fissures, and contact zones of dissolvable and insoluble rock. Two evaluation indexes are selected from hydrological factors, including the groundwater level and rainfall. Two evaluation indexes are selected from anthropogenic factors, including construction disturbance and support measures. Water inrush probability and water inrush quantity are selected as the output of the model. Detailed introduction and risk classification of each evaluation index are shown as follows.

2.3.1. Formation Lithology S_1. The formation lithology mainly refers to the solubility of rock. In references [27, 28], $t=\sum A_iB_j$ is defined for risk classification. Among them, A_i represents solubility (weak solubility, moderate solubility, and strong solubility) and B_j represents the proportions of solute rock in total rock (0–20%, 20%–40%, 40%–60%, and 60%–100%); see Table 1.

2.3.2. Unfavorable Geology S_2. Unfavorable geology usually refers to the water-storing structure in a karst landform, such as cavity, underground river, and karst pipeline. In this paper, risk classification of unfavorable geology is carried out according to the on-site expert assessment, as shown in Table 2 [28].

2.3.3. Topography and Geomorphology S_3. Karst landform is formed by the erosion and deposition of soluble rock by groundwater. Due to the special geological condition of karst

Table 2: Risk classification of unfavorable geology.

Risk classification	Definition
I	High risk: large-sized water-storing structure exists
II	Moderate risk: medium-sized water-storing structure exists
III	Low risk: small-sized water-storing structure exists
IV	No risk: no water-storing structure exists

Table 3: Risk classification of topography and geomorphology.

Risk classification	The proportion of negative relief (%)	Definition
I	>60	Strong water storage capacity
II	30~60	Moderate water storage capacity
III	10~30	Weak water storage capacity
IV	<10	Terrible water storage capacity

landform, plenty of groundwater is accumulated in negative landform, which provides water for water inrush. In reference [35], the proportion of negative landform in the area is used to classify the risk, as shown in Table 3.

2.3.4. Groundwater Table S_4. The quantitative analysis of groundwater table risk classification is the premise of accurate risk assessment [36]. Distance h between the groundwater table and the tunnel floor is used to classify the risk, as shown in Table 4.

2.3.5. Rainfall S_5. According to the rainfall division of meteorology, rainfall in 24 hours l (mm) is used to classify the risk. Because different types of karst tunnels have different response times to rainfall, the time range is set as one week, that is, as long as the rainfall reaches light rain once within a week, the rainfall of this week can be identified as light rain, as shown in Table 5 [29].

2.3.6. Attitude of Rock S_6. The attitude of rocks can indirectly affect the recharge, runoff, and discharge capacity of groundwater. In this paper, the dip angle is used to classify the risk, as shown in Table 6 [36].

2.3.7. Inter-Layer Fissure S_7. The development degree of interlayer fissure represents the activity of groundwater. In reference [29], the development degree of interlayer fissure is used to classify the risk, as shown in Table 7.

2.3.8. Contact Zone of Dissolvable and Insoluble Rock S_8. The contact zone of dissolvable and insoluble rock [5] is a necessary condition for the formation of the underground water-storing structure. The degree of contact zone development is used to classify the risk, as shown in Table 8.

Table 4: Risk classification of contact zones of the groundwater table.

Risk classification	h (m)	Definition
I	≥60	High risk: high water pressure and large instantaneous water inrush quantity
II	30~60	Moderate risk
III	0~30	Low risk
IV	<0	No risk

Table 5: Risk classification of rainfall in a week.

Risk classification	l (mm)	Definition
I	>50	Rainstorm, high risk
II	25~50	Heavy rain, middle risk
III	10~25	Moderate rain, low risk
IV	<10	Light rain or no rain, no risk

Table 6: Risk classification of the attitude of rock.

Risk classification	Attitude of rocks (°)	Definition
I	25~65	Strong water conductivity
II	10~25/65~80	Moderate water conductivity
III	80~90	Weak water conductivity
IV	0~10	Terrible water conductivity

Table 7: Risk classification of interlayer fissures.

Risk classification	Definition
I	The fissure is strongly developed
II	The fissure is generally developed
III	The fissure is poorly developed
IV	The fissure is almost undeveloped

Table 8: Risk classification of contact zones of dissolvable and insoluble rock.

Risk classification	Definition
I	Strongly conducive to the development of large karst structures
II	Generally conducive to the development of large karst structures
III	Poorly conducive to the development of large karst structures
IV	Almost not conducive to the development of large karst structures

2.3.9. Excavation Disturbance S_9. Different excavation methods are used to classify the risk, as shown in Table 9 [37].

2.3.10. Support Measures S_{10}. The support measures of the tunnel are divided into two steps: preliminary support and

Table 9: Risk classification of excavation disturbance.

Risk classification	Definition
I	Blasting excavation, maximum disturbance degree, and range
II	Advance exploratory drilling, general disturbance degree, and range
III	No blasting, minimum disturbance degree, and range
IV	No drilling, no disturbance

Table 10: Risk classification of support measures.

Risk classification	Definition
I	No support, surrounding rock is exposed
II	Preliminary support
III	Secondary reinforcement
IV	Fully support

secondary reinforcement. Therefore, the progress of support measures is used to classify the risk, as shown in Table 10.

2.3.11. Water Inrush Probability and Water Inrush Quantity. Water inrush probability indicates whether water inrush occurred. As the output of the Bayesian network model, it represents the mapping result of each evaluation index on the probability of water inrush; the evidence of division is whether the water inrush would happen, as shown in Table 11 [14].

2.4. Interpretation Structure Model. The interpretative structural modeling method, short for ISM, is a widely used analysis method in modern engineering. ISM can provide the simplest hierarchical topology through mathematical operations without losing system function [34]. The construction steps are as follows.

2.4.1. Determine the Influence Relation Diagram. Twelve indexes ($S_1 - S_{12}$) suitable for the risk assessment model of karst tunnel water inrush have been determined, and the influence diagram of each index is shown in Table 12. In Table 12, A indicates that the horizontal index has influence on the vertical index; B indicates that the vertical index has influence on the horizontal index; C indicates that there is no mutual influence between the two indexes; D indicates that there is mutual influence between the two indexes.

2.4.2. Adjacent Matrix. The adjacency matrix can further reflect the influence relation among various indexes. The transformation formula is shown in formula (2):

$$A = \begin{bmatrix} a_{11} & a_{12} & \cdots & a_{1n} \\ a_{21} & a_{22} & \cdots & a_{2n} \\ \vdots & \vdots & & \vdots \\ a_{n1} & a_{n2} & \cdots & a_{nn} \end{bmatrix},$$

$$S = \{S_i | i = 1, 2, 3 \cdots, n\}. \quad (2)$$

a_{ij} represents the relationship between the index s_i and the index s_j in the adjacency matrix. When $a = 1$, it means that the former has influence on the latter, and when $a = 0$, it means no influence. The transformed adjacency matrix is shown in formula (3):

$$A = \begin{bmatrix} 0 & 1 & 1 & 1 & 0 & 1 & 1 & 1 & 0 & 1 & 1 & 0 \\ 0 & 0 & 0 & 0 & 0 & 0 & 0 & 0 & 0 & 0 & 1 & 1 \\ 0 & 0 & 0 & 1 & 0 & 0 & 1 & 1 & 0 & 0 & 1 & 1 \\ 0 & 0 & 0 & 0 & 0 & 0 & 0 & 0 & 0 & 0 & 1 & 1 \\ 0 & 0 & 0 & 1 & 0 & 0 & 0 & 0 & 0 & 0 & 1 & 1 \\ 0 & 1 & 0 & 1 & 0 & 0 & 0 & 1 & 0 & 0 & 1 & 1 \\ 0 & 1 & 0 & 1 & 0 & 0 & 0 & 1 & 0 & 1 & 1 & 1 \\ 0 & 1 & 0 & 0 & 0 & 0 & 0 & 0 & 0 & 0 & 1 & 0 \\ 0 & 0 & 0 & 0 & 0 & 0 & 0 & 0 & 0 & 1 & 1 & 1 \\ 0 & 0 & 0 & 0 & 0 & 0 & 0 & 0 & 0 & 0 & 1 & 1 \\ 0 & 0 & 0 & 0 & 0 & 0 & 0 & 0 & 0 & 0 & 0 & 0 \\ 0 & 0 & 0 & 0 & 0 & 0 & 0 & 0 & 0 & 0 & 0 & 0 \end{bmatrix}. \quad (3)$$

2.4.3. Accessibility Matrix. Accessibility matrix G is mainly used to describe the degree that can be reached between nodes of the graph. Its calculation formula is shown in formula (4):

$$G = (A + E)^{n+1} = (A + E)^n \neq \cdots \neq (A + E)^2 \neq (A + E). \quad (4)$$

n represents the computation times of matrix A, E is the identity matrix, and the accessibility matrix is in formula (5):

$$G = \begin{bmatrix} 1 & 1 & 1 & 1 & 0 & 1 & 1 & 1 & 0 & 1 & 1 & 1 \\ 0 & 1 & 0 & 0 & 0 & 0 & 0 & 0 & 0 & 0 & 1 & 1 \\ 0 & 1 & 1 & 1 & 0 & 0 & 1 & 1 & 0 & 1 & 1 & 1 \\ 0 & 1 & 0 & 1 & 0 & 0 & 0 & 1 & 0 & 0 & 1 & 1 \\ 0 & 1 & 0 & 1 & 1 & 0 & 0 & 1 & 0 & 0 & 1 & 1 \\ 0 & 1 & 0 & 1 & 0 & 1 & 0 & 1 & 0 & 0 & 1 & 1 \\ 0 & 1 & 0 & 1 & 0 & 0 & 0 & 1 & 0 & 0 & 1 & 1 \\ 0 & 0 & 0 & 0 & 0 & 0 & 0 & 0 & 1 & 1 & 1 & 1 \\ 0 & 0 & 0 & 0 & 0 & 0 & 0 & 0 & 0 & 1 & 1 & 1 \\ 0 & 0 & 0 & 0 & 0 & 0 & 0 & 0 & 0 & 0 & 1 & 0 \\ 0 & 0 & 0 & 0 & 0 & 0 & 0 & 0 & 0 & 0 & 0 & 1 \end{bmatrix}. \quad (5)$$

Table 11: Subgrading of the karst tunnel water irruption quantity.

Subgrading	I		II			III	IV	V
		II_1	II_2	II_3	III_1	III_2		
Water irruption quantity (m^3/h)	≥10000	7000~10000	4000~7000	1000~4000	550~1000	100~550	10~100	≤10

Table 12: Relationship between indexes of karst tunnel water inrush.

S_1	S_2	S_3	S_4	S_5	S_6	S_7	S_8	S_9	S_{10}	S_{11}	S_{12}	
	A	A	A	C	A	A	A	C	A	A	C	S_1
		C	C	C	B	B	B	C	C	A	A	S_2
			A	C	C	A	A	C	C	A	A	S_3
				B	B	B	C	C	C	A	A	S_4
					C	C	C	C	C	A	A	S_5
						C	A	C	C	A	A	S_6
							A	C	A	A	A	S_7
								C	C	A	C	S_8
									A	A	A	S_9
										A	A	S_{10}
											C	S_{11}
												S_{12}

2.4.4. Hierarchical Process. In the accessibility matrix G, the indexes corresponding to the columns with the value of 1 in each row constitute the accessibility set $L(S_i)$ and the indexes corresponding to the rows with the value of 1 in each column constitute the reason set $Q(S_i)$. The necessary and sufficient condition for the variable set O_1 to be the top-level variable set is shown as follows:

$$L(S_i) = L(S_i) \cap Q(S_i). \quad (6)$$

After obtaining set O_1, clear the rows and columns of the indexes corresponding to O_1 in the matrix G, then, get new matrix G, and then, follow the same method, according to formula (6) to get the set O_2, by analogy $O_3, \cdots, O_n$. And finally, form a multistage skeleton matrix structure.

According to the hierarchical process table and the relationship between each index, the interpretation structure model of karst tunnel water inrush risk assessment is shown in Figure 2.

2.5. Correction of the Causality Chart. The causality chart describes the causality among variables through charts, focusing on the results of different combinations of multiple input indexes. Since the interpretation structure model will ignore the skip-level relationship and the important relationship between various indexes, according to the reference, the interpretation structure model is further modified by the causality chart and the final Bayesian network model applied to the risk assessment for water inrush in the karst tunnel is obtained. Figure 3 shows the final Bayesian network model. The new dotted arrows in Figure 3 are used to represent the interaction between each index.

3. The Data Training and Verification of the Bayesian Network Model

After the model is established, Netica software is used to train the model. Firstly, it is necessary to divide each index into interval grades to meet the input and output requirements of the network model; secondly, the engineering cases that can be used for Bayesian network data training need to be counted separately and the interval quantization processing should be carried out; finally, the consistency ratio (RCR) is used to evaluate the training of the model.

3.1. Determine the Input and Output Types of Each Evaluation Index. There are twelve indexes in this model, among which $S_1 - S_{10}$ are the input indexes and $S_{11} - S_{12}$ are the output indexes. The risk classification of the input index is divided into four grades. The output index water inrush probability is divided into two sections, yes and no, and the water inrush quantity is divided into 8 sections to further accurately calculate the disaster consequences. According to the classification of indexes, the intensity of each index is described in Tables 13 and 14.

3.2. Training Specimen of the Network. Bayesian network training requires plenty of data, but the existing databases are all water inrush cases and nonwater inrush cases are not included. If only the existing database is used for

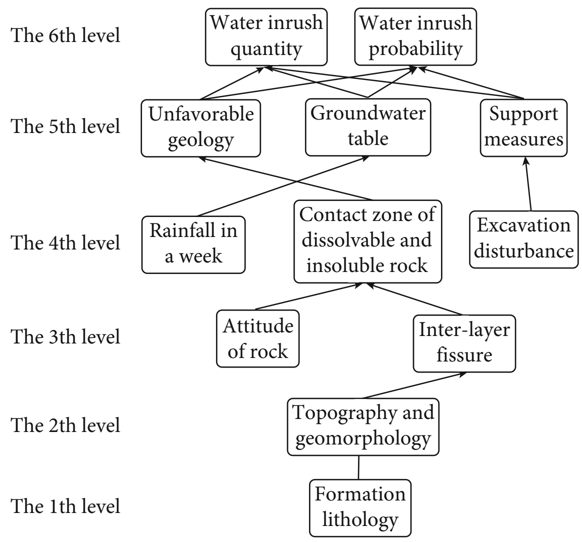

Figure 2: Interpretive structural model among factors of karst tunnel water inrush.

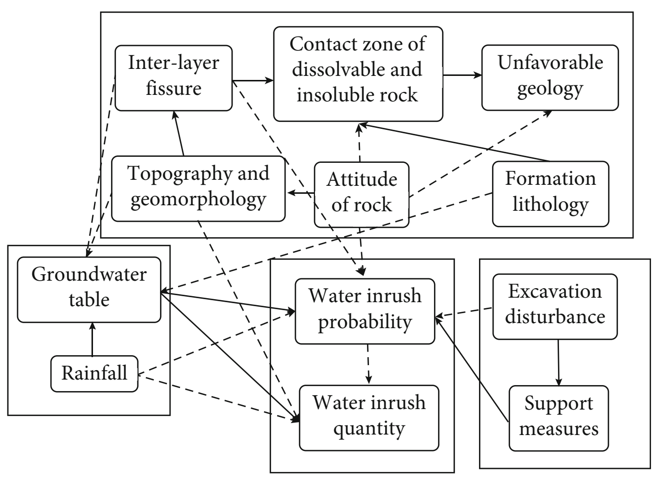

Figure 3: Bayesian network of karst tunnel water inrush.

Table 13: S_1–S_{11} grading interval.

	Strong	Medium	Weak	None
S_1–S_9	I	II	III	IV
S_{10}	IV	III	II	I
	Yes		No	
S_{11}	Yes		No	

The more reasonable the support measures of S_{10}, the lower the risk, so the expression is in contrary to that of the other input indexes.

network training, the sample will be extremely unbalanced. In order to realize the training of the model, based on the idea of generative adversarial network and analytic hierarchy process, some nonwater inrush cases are generated from water inrush cases to further enrich the database.

In essence, the generative adversarial network generates new data according to the existing data range or boundary conditions, which is mainly used to solve problems such as unbalanced database. The process of generating nonwater inrush cases is as follows. Firstly, according to the existing data, S_1, S_2, S_3, S_7, S_8, S_9, and S_{10} are selected and weighted by the analytic hierarchy process and the indexes are quantitatively processed from 0 to 1. Secondly, value range of 0–1 can be obtained by summing the value of each index times the weight, which is denoted as the range of water inrush, that is, if the calculated result is within this range, water inrush disaster will occur. Thirdly, the lower limit of the water inrush range is selected as the boundary between

Table 14: S_{11}–S_{12} grading interval.

	Strong	Medium 1	Medium 2	Medium 3	Weak 1	Weak 2	None 1	None 2
S_{12}	I	II-1	II-2	II-3	III-1	III-2	IV	V

The water inrush quantity is divided into 8 sections corresponding to the subgrading of water irruption quantity in the previous paper.

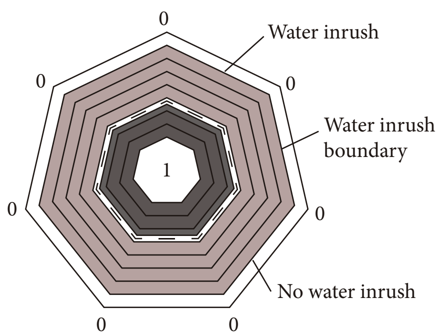

Figure 4: Generative adversarial network diagram.

water inrush and nonwater inrush. According to the one-to-one principle, the nonwater inrush range is obtained from the water inrush range. According to the same weight, it can be calculated backwards to get the corresponding quantitative value between 0 and 1 of each index. Finally, the corresponding grade of each index in nonwater inrush cases can be obtained by reverse mapping from the quantization value. The schematic diagram of the generative adversarial network is shown in Figure 4.

Figure 4 is a seven-sided shape, representing the seven selected indexes. The distance from the corner point to the center is 1, representing the quantitative range of 0–1. The dark-gray area represents the water inrush range, the light-gray area represents the nonwater inrush range, and the dotted line between the two areas represents the water inrush boundary. The judgment matrix constructed by the analytic hierarchy process, as shown in Table 15.

$$\begin{aligned} C &= (0.159, 0.35, 0.07, 0.032, 0.237, 0.106, 0.046), \\ R_{CR} &= \frac{I_{CI}}{I_{RI}} = 0.025 < 0.1. \end{aligned} \tag{7}$$

R_{CR} represents the consistency ratio, and when it is less than 0.1, it represents that the consistency of the judgment matrix meets the requirements; I_{CI} represents the consistency index; I_{RI} represents the average random consistency index.

According to I (0.75–1), II (0.75–0.5), III (0.5–0.25), and IV (0–0.25) to quantify the various samples, 37 water inrush samples are selected from the database for quantitative process and the range of water inrush samples is 0.55–0.9 according to the calculation method of the above-introduced water inrush range . Select 0.5 as the water inrush boundary, and it can be concluded that the nonwater inrush range is 0.1–0.45. According to the reverse calculation method, the corresponding nonwater inrush cases can be obtained. Finally, reverse quantitative processing and the risk classification of each index of the nonwater inrush cases can be obtained.

3.3. Bayesian Network Model Training and Verification Results. Figure 5 shows the training results of the Bayesian network model, and the probability table of each index after training is shown. Ten samples are selected from the database for verification. After verification, the accuracy for water inrush probability is 100% and that for predicting water inrush quantity is 90%.

4. Application of Bayesian Network Risk Assessment Model

The DK490+373 section of the Shanggaoshan Tunnel of the Chengdu-Guiyang Railway is selected to verify the feasibility of the model.

4.1. Engineering Background. The Shanggaoshan Tunnel of the Chengdu-Guiyang Railway is located in Qingzhen city, Guizhou province [38]. The maximum depth of the tunnel reaches 135 m. The average annual rainfall reaches 1000–1600 mm. The surrounding rock of the DK490+373 section is mainly composed of limestone, marl, and other carbonate rocks, and the overall dip angle of the rock layer is 5°–30°. Rock joints and fractures most are open and vertical.

4.2. The Determination of Input Indexes. According to the engineering data, the Bayesian network model is used to predict the water inrush risk of DK490+373 of the Shanggaoshan Tunnel under no-rain and heavy-rain conditions. Risk classification of each input index is shown in Table 16.

There is no accurate quantitative data to describe the topography and geomorphology, formation lithology. According to the description of engineering data and the risk classification of the index, it is considered as moderate risk. The overall dipping direction is 5°–30°; according to the abovementioned risk classification, the attitude of rocks is considered as moderate risk. The water storage structures in the tunnel area mainly are karst pipeline and small karst cave, which are classified as moderate risk. According to the engineering data, interlayer fissure is classified as moderate risk by qualitative description. The bench cut method is adopted in construction, and water inrush occurred without support, so it can be concluded that the construction disturbance is weaker than blasting but stronger than drilling. Due to the lack of support measure, it can be determined as high risk.

4.3. Prediction Result of the Bayesian Network Risk Assessment Model. Figure 5 shows the training result of the Bayesian network model. Input the values of the indexes in

Table 15: Overview of the value of each input index.

	Topography and geomorphology	Contact zones of dissolvable and insoluble rock	Formation lithology	Unfavorable geology	Interlayer fissure
No rainfall	II (medium)	*	II (medium)	II (medium)	II (medium)
Heavy rainfall	II (medium)	*	II (medium)	II (medium)	II (medium)
	Attitude of rock	Groundwater table	Rainfall in a week	Excavation disturbance	Support measures
No rainfall	II (medium)	*	IV (none)	II (medium)	IV (strong)
Heavy rainfall	II (medium)	*	II (medium)	II (medium)	IV (strong)

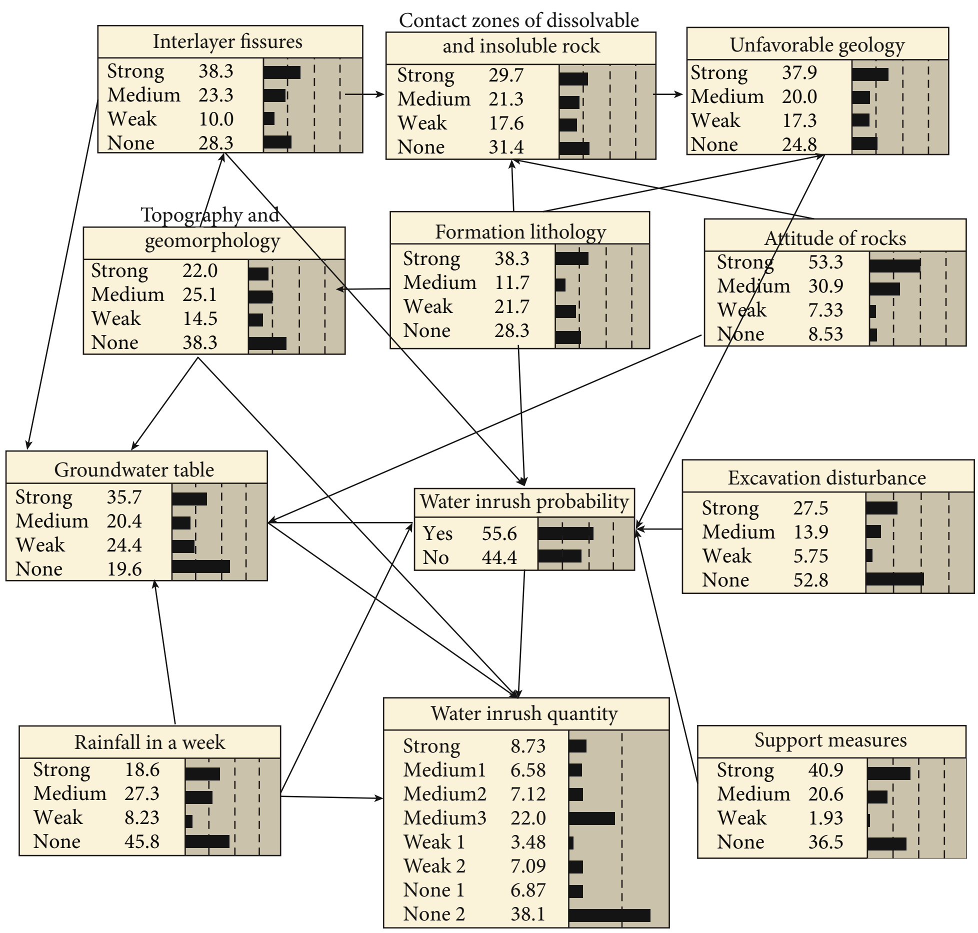

Figure 5: Bayesian network training results.

Table 16 in turn, and observe whether the final output is consistent with the reality. In the case of no rain or heavy rain, the prediction results of water inrush in the DK490 +373 section are shown in Table 17.

4.4. Realistic Water Inrush Situation. On the 23th of August, 2015, the exit section of the tunnel was excavated to DK490 +373 and a karst cave with diameter of 0.55 m was exposed at the right-side wall. Small-scale water inrush occurred immediately, and water inrush quantity reaches 226.8m^3/h. After investigation, it was found that the exposed karst cave was connected with the karst pipe, which resulted in the continuous small-scale water inrush. The geological profile of the section is shown in Figure 6. On the 28th of August, 2015, massive sustained rainfall (the rainfall in 24 hours reached 33.4 mm, which can be identified as heavy rain) occurred within the tunnel area, which caused large-scale water inrush disaster in the tunnel, with the water inrush quantity reaching 5005 m^3/h.

4.5. Results Analysis. Under the condition of heavy rain or no rain, the prediction results of water inrush risk in section

Table 16: Overview of the value of each input index.

	Topography and geomorphology	Contact zones of dissolvable and insoluble rock	Formation lithology	Unfavorable geology	Interlayer fissure
No rainfall	II (medium)	*	II (medium)	II (medium)	II (medium)
Heavy rainfall	II (medium)	*	II (medium)	II (medium)	II (medium)
	Attitude of rock	Groundwater table	Rainfall in a week	Excavation disturbance	Support measures
No rainfall	II (medium)	*	IV (none)	II (medium)	IV (strong)
Heavy rainfall	II (medium)	*	II (medium)	II (medium)	IV

*The value of the index is unknown, such as contact zones of dissolvable and insoluble rock and groundwater table.

Table 17: Prediction and real result.

	Prediction result		Actual result	
	Probability of water inrush	Water inrush quantity	Whether water inrush occurs	Water inrush quantity
No rainfall	85.3%	100~550 m^3/h	Yes	226.8 m^3/h
Heavy rainfall	51.3%	4000~7000 m^3/h	Yes	5005 m^3/h

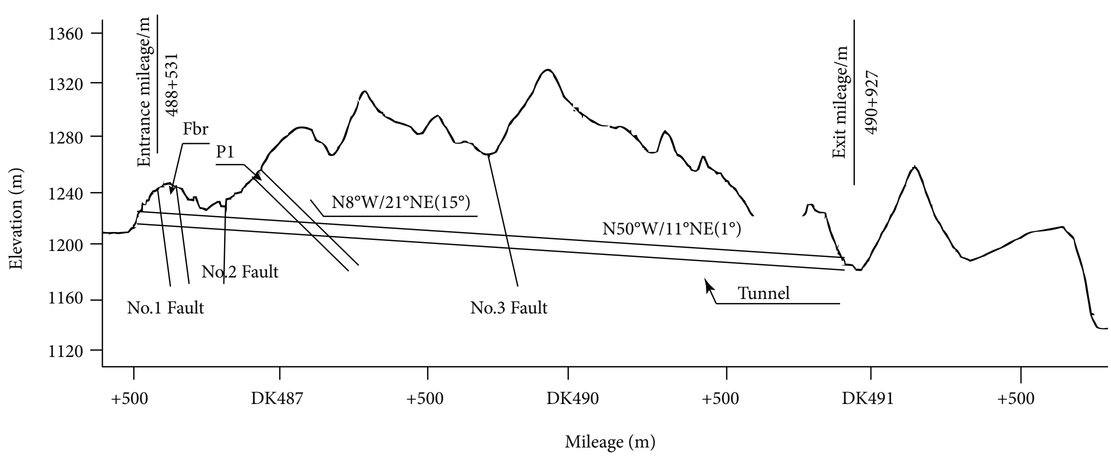

Figure 6: Geological section of Shanggaoshan Tunnel.

DK490+373 are completely consistent with reality. It can be seen from the results that this model is accurate and practical in predicting karst tunnel water inrush probability and quantity.

5. Conclusion

Based on the Bayesian theory, interpretive structure model, generative adversarial networks, and analytic hierarchy process, a new Bayesian network risk assessment model is established. The main conclusions are as follows:

Twelve indexes which can not only characterize the karst tunnel water inrush but also are easy to be counted are selected as the input and output indexes of the model, which summarizes the disaster-causing factors of karst tunnel water inrush comprehensively and effectively improves the accuracy of the Bayesian risk assessment model.

In view of the variability and complexity of the underground engineering environment, a new Bayesian network risk assessment model is established. The model overcomes the shortcomings of other risk assessment models that rely too much on geological data. Through massive data learning, it can carry out accurate risk assessment under the condition of incomplete geological data and unknown disaster cause.

Based on the idea of the generative adversarial network and principle of the analytic hierarchy process, the generation method of no water inrush samples is proposed for the first time, which can generate no water inrush sample from water inrush sample database, and effectively solved the problem of unbalanced database.

The Bayesian network risk assessment model is applied to the risk assessment of water inrush in the DK490+373 section of the Shanggaoshan Tunnel. The result shows that the model is operable, effective, practical, and also applicable to the case of incomplete index statistics. The prediction results of water inrush risk are completely consistent with the realistic water inrush situation.

Data Availability

The data used to support the findings of this study are available from the corresponding author upon request.

Conflicts of Interest

The authors declare that they have no conflicts of interest.

Acknowledgments

Support provided by the open research fund of the State Key Laboratory of Geomechanics and Geotechnical Engineering, Institute of Rock and Soil Mechanics, Chinese Academy of Sciences (no. Z020014), the Key Research and Development Program (Social Development) of Xuzhou City (KC21298), and the National Natural Science Foundation of China (no. 41572263) are sincerely acknowledged.

References

[1] D. Ma, *Study on Impact Mechanism of Deep Buried Karst to Tunnel Safety and the Treatment Technique, [Ph.D. Thesis]*, Beijing Jiaotong University, 2012.

[2] J. L. Wilson, "Characteristics of carbonate-platform margins," *American Association of Petroleum Geologists Bulletin*, vol. 58, no. 5, pp. 810–874, 1974.

[3] L. P. Li, T. Lei, S. C. Li et al., "Risk assessment of water inrush in karst tunnels and software development," *Arabian Journal of Geosciences*, vol. 8, no. 4, pp. 1843–1854, 2015.

[4] W. Lu, Z. Zhou, T. Liu, and Y. H. Liu, "Discrete element simulation analysis of rock slope stability based on UDEC," *Advanced Materials Research*, vol. 461, pp. 384–388, 2012.

[5] Y. C. Wang, F. Geng, S. Q. Yang, H. Jing, and B. Meng, "Numerical simulation of particle migration from crushed sandstones during groundwater inrush," *Journal of Hazardous Materials*, vol. 362, pp. 327–335, 2019.

[6] Y. C. Wang, H. W. Jing, H. J. Su, and J. Xie, "Effect of a fault fracture zone on the stability of tunnel-surrounding rock," *International Journal of Geomechanics*, vol. 17, no. 6, 2017.

[7] N. Zhao, Y. C. Wang, B. Meng, and N. Luo, "Numerical simulation on the seepage properties of soil-rock mixture," *Advances in Materials Science and Engineering*, vol. 2018, Article ID 1859319, 10 pages, 2018.

[8] S. V. Kuznetsov and V. A. Trofimov, "Hydrodynamic effect of coal seam compression," *Journal of Mining Science*, vol. 38, no. 3, pp. 205–212, 2002.

[9] M. Salis and L. Duckstein, "Mining under a limestone aquifer in southern Sardinia: a multiobjective approach," *International Journal of Mining Engineering*, vol. 1, no. 4, pp. 357–374, 1983.

[10] S. C. Li, C. L. Gao, and Z. Q. Zhou, "Analysis on the precursor information of water inrush in karst tunnels: a true triaxial model test study," *Rock Mechanics & Rock Engineering*, vol. 52, p. 2, 2019.

[11] F. Chen, Y. C. Wang, W. Jiang, and S. H. Zheng, "Numerical simulation of ground movement induced by water and sand gushing in subway through fault based on DEM-CFD," *Computers and Geotechnics*, vol. 139, article 104282, 2021.

[12] Y. C. Wang, F. Chen, X. Z. Li, X. Yin, F. Geng, and S. H. Zheng, "Experimental Investigation on Mass Loss Characteristics of Broken Rocks with Discontinuous Gradation," *International Journal of Geomechanics*, vol. 21, no. 9, p. 04021168, 2021.

[13] Y. C. Wang, Z. Y. Li, H. W. Jing, Y. B. Li, and M. T. Wang, "Study on the seepage characteristics of deep buried tunnels under variable high-pressure water heads," *Bulletin of Engineering Geology and the Environment*, vol. 80, no. 2, pp. 1477–1487, 2021.

[14] S. C. Li, P. He, L. P. Li et al., "Reliability analysis method of sub-classification of tunnel rock mass and its engineering application," *Rock and Soil Mechanics*, vol. 39, no. 3, pp. 967–976, 2018.

[15] G. F. Salazar, *Stochastic and Economic of Adaptability in Tunneling Design and Construction*, Department of Civil Engineering, Massachusetts Institute of Technology, Cambridge, MA, USA, 1983.

[16] G. Z. Ou, Y. Y. Jiao, G. H. Zhang, J. P. Zou, F. Tan, and W. S. Zhang, "Collapse risk assessment of deep-buried tunnel during construction and its application," *Tunnelling and Underground Space Technology*, vol. 115, no. Sep 2021, p. 104019, 2021.

[17] Z. H. Peng, L. W. Chen, X. W. Hou, Q. H. Ou, J. Zhang, and Y. F. Chen, "Risk assessment of water inrush under an unconsolidated, confined aquifer: the application of Gis and information value model in the Qidong coal mine, China," *Earth Science Informatics*, vol. 14, no. 4, pp. 2373–2386, 2021.

[18] W. F. Tu, L. P. Li, S. Cheng, D. Y. Chen, Y. C. Yuan, and Y. H. Chen, "Evolution mechanism, monitoring, and early warning method of water inrush in deep-buried long tunnel," *Geofluids*, vol. 2021, Article ID 2023782, 16 pages, 2021.

[19] H. C. Yin, B. Xu, S. X. Yin, W. Z. Tian, H. Yao, and H. P. Meng, "Prevention of water inrushes in deep coal mining over the Ordovician aquifer: a case study in the Wutongzhuang Coal Mine of China," *Geofluids*, vol. 2021, Article ID 5208670, 13 pages, 2021.

[20] J. N. Yin, F. T. C. Tsai, and S.-C. Kao, "Accounting for uncertainty in complex alluvial aquifer modeling by Bayesian multimodel approach," *Journal of Hydrology*, vol. 601, article 126682, 2021.

[21] G. D. Zhang, Y. G. Xue, C. H. Bai, M. X. Su, K. Zhang, and Y. F. Tao, "Risk assessment of floor water inrush in coal mines based on Mfim-Topsis variable weight model," *Journal of Central South University*, vol. 28, no. 8, pp. 2360–2374, 2021.

[22] J. Pearl, *Probabilistic Reasoning in Intelligent Systems: Networks of Plausible*, Morgan Kaufmann, 1988.

[23] J. S. Wu, Y. P. Bai, W. P. Fang, R. Zhou, G. Reniers, and N. Khakzad, "An integrated quantitative risk assessment method for urban underground utility tunnels," *Reliability Engineering & System Safety*, vol. 213, article 107792, 2021.

[24] B. Nilsen, A. Palmström, and H. Stille, "Quality control of a subsea tunnel project in complex ground conditions," in *Proceedings of the ITA World Tunnel Congress*, pp. 137–145, Oslo, NO, USA, 1992.

[25] J. Kampmann, S. D. Eskesen, and J. W. Summers, "Risk assessment helps select the contractor for the Copenhagen Metro System," *Proceedings of the world tunnel congress 98 on tunnels and me-tortoises*, vol. 98, pp. 123–128, 1998.

[26] E. H. Weiss and L. Vig, “Mediation-A proper tool for risk assessment in tunneling projects,” in *Proceedings of the AITE-SITA 2001 world tunnel congress*no. 3, pp. 583–588, 2001.

[27] Y. C. Wang, H. W. Jing, L. Y. Yu, H. J. Su, and N. Luo, “Set pair analysis for risk assessment of water inrush in karst tunnels,” *Bulletin of Engineering Geology and the Environment*, vol. 76, no. 3, pp. 1199–1207, 2017.

[28] Y. C. Wang, X. Yin, F. Geng, H. W. Jing, H. J. Su, and R. C. Liu, “Risk assessment of water inrush in karst tunnels based on the efficacy coefficient method,” *Polish Journal of Environmental Studies*, vol. 26, no. 4, pp. 1765–1775, 2017.

[29] D. S. Hou, X. Zhang, and L. Wang, “Risk evaluation of tunnel water inrush based on comprehensive weighting-TOPSIS method and its application,” *Tunnel Construction*, vol. 37, no. 6, pp. 691–699, 2017.

[30] J. L. Hu, X. W. Tang, and J. N. Qiu, “A Bayesian network approach for predicting seismic liquefaction based on interpretive structural modeling,” *Georisk Assessment & Management of Risk for Engineered Systems & Geohazards*, vol. 9, no. 3, pp. 200–217, 2015.

[31] J. J. Kool, W. Kanning, C. Jommi, and S. N. Jonkman, “A Bayesian hindcasting method of levee failures applied to the Breitenhagen slope failure,” *Georisk-Assessment and Management of Risk for Engineered Systems and Geohazards*, vol. 15, no. 4, pp. 299–316, 2021.

[32] T. Y. Zhao, J. Y. Lei, and L. Xu, “An efficient Bayesian method for estimating runout distance of region-specific landslides using sparse data,” *Georisk-Assessment and Management of Risk for Engineered Systems and Geohazards*, vol. 16, no. 1, pp. 140–153, 2022.

[33] X. Hu, *Risk Analysis for High-Speed Rail Karst Tunnel Based on the Bayesian Network, [M.S. thesis]*, Hunan University Of Science And Technology, 2014.

[34] X. W. Tang, J. L. Hu, and J. N. Qiu, “Identifying significant influence factors of seismic soil liquefaction and analyzing their structural relationship,” *KSCE Journal of Civil Engineering*, vol. 20, no. 7, pp. 2655–2663, 2016.

[35] S. C. Li, Z. Q. Zhou, L. P. Li, S. S. Shi, and Z. H. Xu, “Risk evaluation theory and method of water inrush in karst tunnels and its applications,” *Chinese Journal of Rock Mechanics and Engineering*, vol. 32, no. 9, pp. 1858–1867, 2013.

[36] L. P. Li, S. C. Li, J. Chen, J. L. Li, Z. H. Xu, and S. S. Shi, “Construction license mechanism and its application based on karst water inrush risk evaluation,” *Chinese Journal of Rock Mechanics and Engineering*, vol. 30, no. 7, pp. 1345–1355, 2011.

[37] X. Yin, J. X. Ye, and Y. C. Wang, “Analysis of water inrush mode and quantitative analysis of influence factors of deep buried karst tunnel,” *Bulletin of Science and Technology*, vol. 34, no. 4, pp. 247–253, 2018.

[38] Z. H. Fang, Y. Yang, and H. J. Ding, “Study on water gushing disease of karst pipeline in Shanggaoshan Tunnel of Chengdu-Guiyang Railway,” *High Speed Railway Technology*, vol. 8, no. 4, pp. 70–73, 2017.